

COMMISSIONING OF THE NEW SARAF RFQ AND DESIGN OF THE NEW LINAC

A. Perry, D. Berkovits, H. Dafna, B. Kaizer, Y. Luner, J. Rodnizki, A. Shor, I. Silverman,
L. Weissman, Soreq Nuclear Research Center, Yavne, Israel
R. Duperrier, G. Ferrand, B. Gastineau, M. Jacquemet, S. Ladegaillerie, C. Madec, N. Pichoff,
T. Plaisant, D. Uriot CEA/IRFU, Gif-sur-Yvette, France
A. Bechtold, P. Niewieczerzal Neue Technologien GmbH, Gelnhausen, Germany

Abstract

Soreq Nuclear Research Center (SNRC) and CEA collaborate for the upgrade of the existing Soreq Applied Research Accelerator Facility (SARAF) accelerator up to 5mA Continuous Wave (CW) 40 MeV deuteron and proton beams (Phase 2). SNRC is upgrading the injector: the ion source, the low energy beam transport line and the 4-rods Radio Frequency Quadrupole (RFQ). CEA is in charge of the development and commissioning of the medium energy beam transport line and the superconducting linac. This paper presents the status of the SARAF linac development by CEA and the installation and testing of a new set of rods electrodes in the SARAF RFQ.

INTRODUCTION

Soreq Applied Research Accelerator Facility (SARAF) is based on a high intensity proton/deuteron linac currently in operation at Soreq Nuclear Research Center (SNRC, Israel) [1]. SARAF-Phase 2 project aims to upgrade the existing capabilities and, in particular, increase the available beam energy and current up to 40MeV and 5mA respectively, in both pulsed and Continuous Wave (CW) modes.

Within the frameworks of the Phase 2 project, CEA (France) manages the SARAF-LINAC project [2]. This project includes the design, construction and commissioning of a new Medium Energy Beam Transport (MEBT) line and a new Superconducting Linac (SCL) made of 4 cryomodules (CM1-CM4). These will replace the existing MEBT and Prototype Superconducting Module (PSM) which are now in operation. The SARAF-LINAC project is now approaching the end of its third and final year of detailed design and prototyping, and is about to transition into the production stage. In preparation, several design reviews took place in 2018. The status of the SARAF-LINAC project will be presented in the second part of this paper.

The existing ion source, Low Energy Beam Transport (LEBT) line and Radio Frequency Quadrupole (RFQ) will serve as the injector to the Phase 2 linac. SNRC is modifying these components in order to reach the Phase 2 specifications. In particular, significant efforts have been devoted to improving the RFQ performance. The original SARAF RFQ, designed by the University of Frankfurt [3] and built by NTG GmbH and RI-ACCEL GmbH, has been able to accelerate high intensity (up to 4 mA) proton beams to 1.5 MeV. However, despite numerous conditioning campaigns, acceleration of CW deuteron beams in the RFQ was

unachievable for a long time. Over the years a series of major modifications to the RFQ structure have led to a considerable improvement of the RFQ performance and, following the introduction of an additional RF power coupler, record results of high power operation were achieved in April 2016 [4]. Yet, reliable CW operation at the 250 kW power level which was required for CW deuteron acceleration was unachievable. It was therefore decided to re-design the rods modulation in order to enable deuteron acceleration at a slightly lower inter-electrode voltage [5]. Lowering of the applied RFQ voltage, while keeping the RFQ length and the entrance beam properties, has the unavoidable consequence of lowering the inter-rod separation and lowering the outgoing beam energy from 1.5 MeV/u to 1.27 MeV/u. Extensive beam dynamics simulations of the redesigned RFQ were performed using the GPT beam dynamics code [6] and showed that the beam quality in the transverse and longitudinal phase space should improve with the new modulation. Further simulations using the TraceWin code package [7] indicated that the beam emerging from the RFQ can be satisfactorily matched to the SCL. Electromagnetic simulations using CST [8] were performed as well to guarantee proper RF resonance frequency and to estimate the field homogeneity in the structure. Following this work the new rods fabrication was performed at Neue Technologien (NTG).

INSTALLATION OF THE NEW RODS

Installation of the electrodes was accomplished in two sessions utilizing a laser tracking system. The RFQ tank was opened and the old rods and tuning plates were disassembled and stored prior to the first laser tracker session, which focused on measurements of the stems heights. On the basis of these measurements and the metrology of the electrodes a set of precise shims spacers was manufactured to compensate for errors on stems and electrodes. The new electrodes were installed in their positions with the adapted shims during the second installation campaign (June 2017). The top and side positions of all electrode supports were measured. The measuring positions are indicated as red spots in Fig. 1. As seen in Fig. 1 the deviations of the measured and calculated positions are within ± 40 and ± 10 microns for the top and side surfaces respectively.

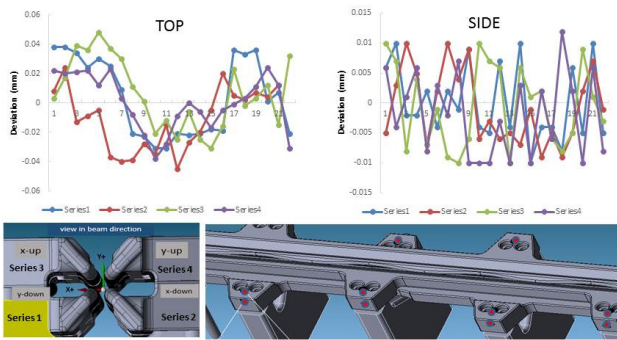


Figure 1: Deviations between the measured and calculated positions of the top and side surfaces of the installed new rods. The red spots indicate the measured positions.

The tuning plates had to be installed after the installation of the electrodes to adjust the resonance frequency and the field homogeneity. At first 15 dummy plates made of aluminium were mounted in between the stems into initial calculated positions. The resonance frequency and the field distribution were brought to the optimum via an iterative procedure (Fig. 2). The field distribution was measured by means of the perturbation method. After determination of the optimum tuning plates positions the dummy tuning blocks were replaced by the newest generation high power tuning plates (made of copper covered by a silver plate). Fine tuning of the plates positions was performed based on additional field measurements. In the final state the resonance frequency, with the RFQ plunger tuners positioned in the middle of their tuning range, was 175.943 MHz in air or 175.986 MHz in vacuum. The final field non homogeneity was around 1.8 % (standard deviation). For comparison the corresponding number for the old structure was 2.7 %, which could only be achieved by a deliberate re-positioning of the rods towards the high energy end in order to change the capacitance.

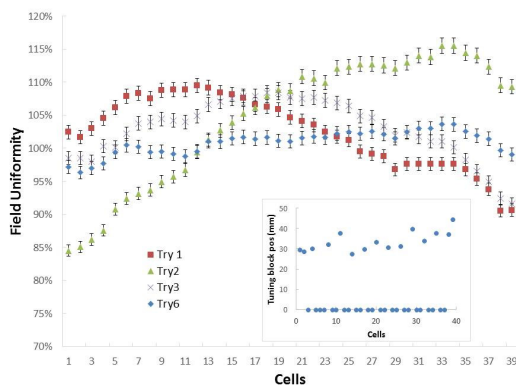


Figure 2: Iterative procedure for tuning the field homogeneity. The final position of the tuning plates is indicated in the inset.

HIGH POWER CONDITIONING

The first tests with proton beams (described in the following section) indicated that the new RFQ structure is performing well within the designed parameters and that the power required for deuteron operation would be 180-

190 kW. Hence the goal for the conditioning campaign was set to ~200 kW.

It took five operational days (36 net hours) to reach 180 kW RF power (Fig. 3, left). In the first day only low duty cycle (<1 %) was used to bring the pulsed forward power to the 200 kW level. During the consecutive four days the pseudo CW duty cycle (> 99%) was used and the RF power was gradually increased. Relatively fast progress can be explained by all the recent modifications. In addition a digital reflection protection box was used for the first time instead of a similar analog device. The reflected power measured by the directional coupler was analysed and introduced in an FPGA processor. In case of high reflected power the FPGA processor switched off the input signal to the RF amplifier for a pre-determined period (usually ~60 msec), allowing for a discharge event to decay. Utilization of the protection box is the main reason for performing conditioning in the pulsed pseudo CW mode rather than real CW operation.

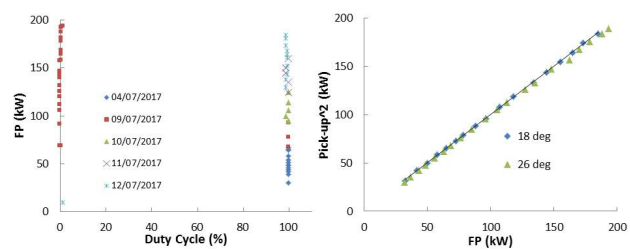


Figure 3: Left. The progress of the first stage of high power conditioning. Right. Dependence of the normalized square of the pick-up amplitude versus the forward power taken for two temperatures of the cooling water.

The final stage of the high power conditioning spanned four days (33 net hours). At the end of this period we were able to keep RFQ: at 195 kW CW for many hours without a single trip and at 205-210 kW CW at the trip rate of one per hour. The dependence of the electrical field (measured using a pick-up antenna) on the forward power is shown in Fig. 3, right. A deviation from linearity may be an indication of ‘dark currents’ in the RFQ. However, the measurements demonstrate that there is no measurable loss of RF power up to the highest used power values.

BEAM COMMISSIONING

The next stage of the RFQ commissioning entailed detailed beam characterization using the SARAF diagnostic plate (D-plate), which is positioned after the SARAF cryomodule. This configuration considerably hindered the measurement of some beam properties at the RFQ exit. Accurate measurements of the beam energy were done using the Rutherford backscattering (RBS) of beam particles off a thin gold foil introduced into the beam halo [9]. The results of energy measurements for proton and deuteron beams as a function of RF power are displayed in Fig. 4. The obtained beam energy is about 1.275 keV and 2.555 keV for protons and deuterons correspondingly which is very close to the designed values.

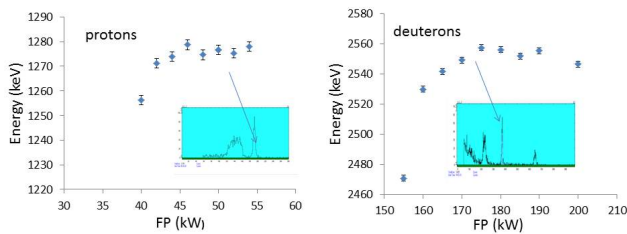


Figure 4: RBS measurement of beam energy as a function of the RF power for protons (Left) and deuterons (Right) are presented. The RBS spectra are shown in the inserts.

Transverse emittance measurements were performed using vertical and horizontal slit-wire sets at the D-plate. The measurements were done with beam pulses of 0.5 ms of protons and deuterons and for various intensities up to 5.5 mA while the RFQ field was operated in CW. The measured values of the normalized rms emittances are within the specifications for both protons and deuterons ($\sim 0.2 \pi\text{-mm-mrad}$). The measured projections of a 5mA deuteron beam are depicted in Fig. 5. The measured RMS emittance in this case was $0.14/0.23 \pi \text{ mm mrad}$ in the horizontal/ vertical direction respectively.

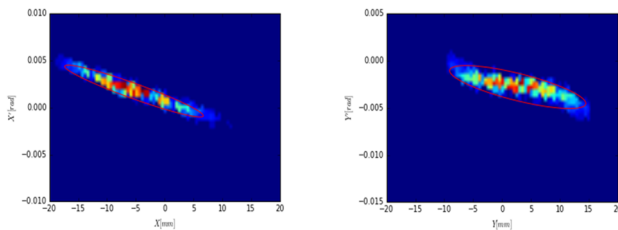


Figure 5: Slit-wire measurements (at the D-plate) of the transverse phase space projections for a 5 mA deuteron beam. The red ellipse is the $4 \times \text{RMS}$ ellipse.

The RFQ transmission was measured by comparing the current readings at the LEBT and the D-plate Faraday cups. The dependence of the transmission values on the input beam current is compared for the old and new rod structures in Fig. 6. The present and the previous (December 2015) measurements were performed in the same manner - only the ion source magnetron RF power was changed to vary the LEBT current and all the LEBT optical parameters were kept the same, except for fine tuning of the last LEBT solenoid. It is seen in Fig. 6 that the RFQ transmission has improved slightly for the proton beam, although the general trend of the transmission reduction with increase of the current persisted. There is also a modest increase of the transmission for deuterons for the new rod structure. Moderate improvement in RFQ transmission took place in spite of the fact that the physical aperture area between the new rods was reduced effectively by 30%. The improvement is due, in part, to a smoother gentle bunching section and, in part, to a constant aperture in the accelerating region, as well as due to the improved field homogeneity achieved with the new rod structure.

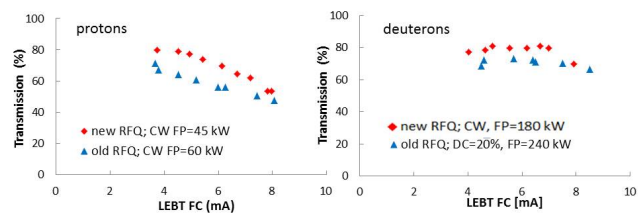


Figure 6: The RFQ transmission as a function of the input current for protons (left) and deuterons (right). Measurements for the new and old rod structures are compared.

Beam dynamics simulations of the phase 2 linac show that the longitudinal emittance of the beam formed by the RFQ is an important parameter. To measure it, the gradient variation technique was invoked in a similar fashion to that described in [10]. During the measurement three superconducting cavities in the PSM were operated. The last cavity was operated as a buncher and its voltage was varied. The beam energy spread was measured using the RBS apparatus for each voltage setting and the RMS emittance was then extracted from the measurements, as shown graphically in Fig. 7. The result, after correcting for an estimated $\sim 20\%$ emittance growth during the transport to the D-plate, is $\sim 1.1 \pi\text{-keV/u-nsec}$.

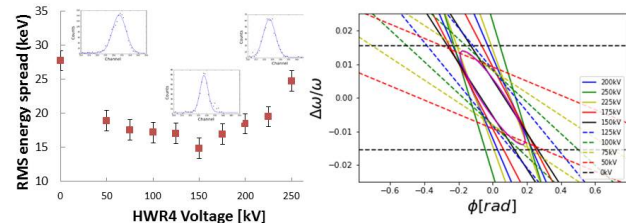


Figure 7: Left - The results of energy distribution measurement are presented. Some examples of spectra are shown in the insets. Right - The phase space ellipse obtained from the RBS measurements.

Finally, demonstration of CW deuteron operation is an important milestone of SARAF Phase I which was overdue for a decade. The test, performed in October 2017, started with acceleration of a low duty cycle beam while the RFQ was working in CW mode at 190 kW. The cryogenic cavities were detuned and the beam was stopped at the beam dump after the D-plate. The pulse intensity was kept at 1.15 mA. The duty cycle was gradually increased using the slow chopper to 99.5% while monitoring vacuum in the cavities and cryogenics. After reaching the pseudo CW level RFQ was operational for half an hour smoothly until an RFQ trip. Operation of deuteron beam in CW mode is feasible now with the upgraded RFQ structure.

THE SARAF LINAC PROJECT

The components of SARAF-LINAC are planned to be installed and commissioned in 3 phases in: 2020 (MEBT), 2021 (CM1) and 2022 (CM2-4) [2].

Content from this work may be used under the terms of the CC BY 3.0 licence (© 2018). Any distribution of this work must maintain attribution to the author(s), title of the work, publisher, and DOI.

System

A systematic engineering process is applied to derive and monitor requirements, specifications, solutions and acceptance of each subsystems (from SARAF-LINAC system to small components sub-systems).

The proton or deuteron beam dynamics, from 40 μ A to 5 mA, from 1.3 MeV/u to 40 MeV final energy have been calculated (including the error studies) with TraceWin code package [11]. The linac tuning strategy [12] and associated performances [7], mainly focused on beam losses (Fig. 8), have been studied.

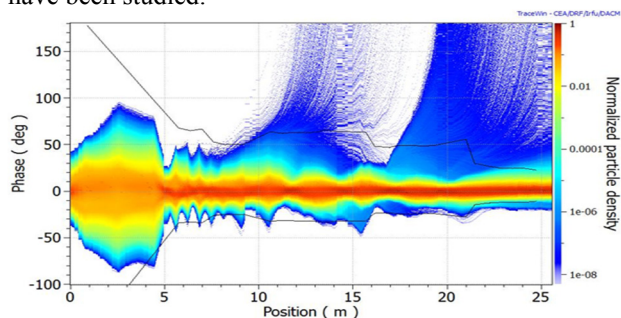


Figure 8: Beam statistical longitudinal distribution with errors. Blue tails represent unhooked particles with very low probability ($<10^{-7}$).

Major Component Status

The major components prototypes or first of series are being built and tested:

- MEBT Rebunchers by SDMS company [13],
- HWR by RI company [14],
- RF Couplers by TETD company [15],
- Solenoid Packages by ELYTT [16] and CRIOTEC [17] companies.

The associated test stands are getting prepared for acceptance tests planned in the second semester of 2018.

In parallel, cryomodules just passed their CDR and enter in call for tender process.

The MEBT Rebuncher



Figure 9: First rebuncher @ SDMS.

The three 105 kV CW, 5 kW, $\beta=0.053$ NC rebunchers (RB1-3) are being built by SDMS Company. Acceptance

tests of RB1 (vacuum performances, water leaks, frequency tuning (geometry)) before copper coating (Fig. 9) are planned in mid-September @ SDMS. The validation will lead to RB1 copper coating and RB2&3 start of manufacturing. Once copper coated, the RB1 has to be validated (power consumption, cooling performances) at IRFU at early 2019 before copper coating of RB2&3.

The SC HWR

The bare low-beta (0.091) prototype has been built by RI Company. It has been prepared (BCP, HPR) and tested @ 4.5 K by CEA. Multipactor at low and medium fields has been observed and passed through. The measured surface resistance at low field is 15 nOhms (requirement: < 45 nOhm @ 7 MV/m). Maximum accelerating field of 10.6 MV/m has been achieved without X-rays and quench (7 MV/m specified, 6.5 MV/m required). As shown on Fig. 10, a Q-slope is observed leading to a Q0 that is a little bit lower than the specified one (at 7 MV/m).

The high-beta (0.181) prototype is being built by RI. The bare cavity should be delivered to CEA for preparation within one month.

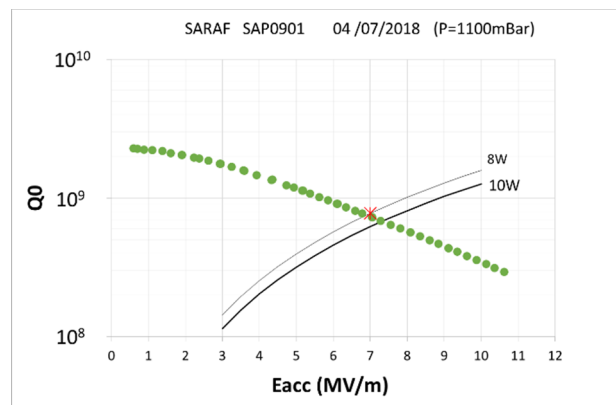


Figure 10: LB HWR prototype results.

The RF couplers

The first 2 RF couplers have just been delivered to IRFU (Fig. 11). They will be conditioned/tested on specific test stand (C2TS) next month.



Figure 11: Coupler 1 prototype (photo by TETD).

The SC Magnet

The Final Design Review of SC magnets has been done at the ELYTT Company's manufacturing site. The prototype is now under construction. The delivery is expected in October

The Current Lead Cluster

The Current Lead Clusters, designed by CEA, are being manufactured by CRIOTEC Company (see Fig. 12).

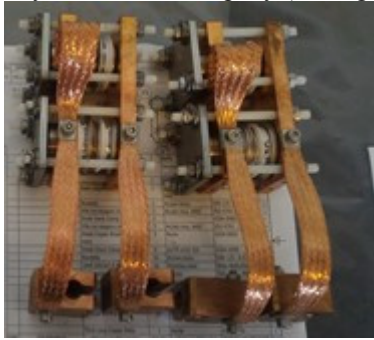


Figure 12: Current lead protection (photo by CRIOTEC).

The Cryomodules

The ~5 m long cryomodules (Fig. 13) of 2 different types (CM1-2, for LB HWR and CM3-4 for HB HWR) passed their CDR in March [18]. The technical specifications for the call for tenders of their components are being written.

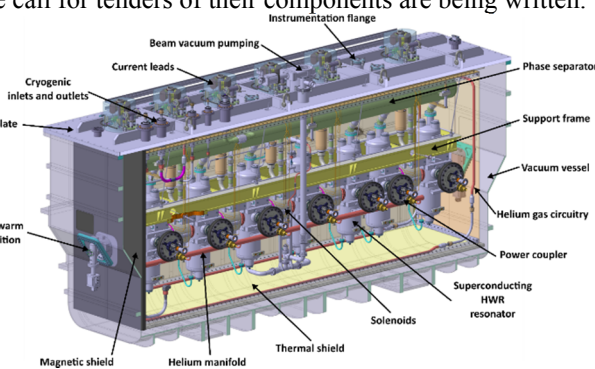


Figure 13: CM2 3D mock-up.

TEST STANDS

The major components will be tested at IRFU in dedicated test stands (TS) all in the same facility (Fig. 14):

- RBTS for Rebunchers.
- VCTS for Vertical Cavities,
- ECTS for Equipped Cavities (with coupler and tuner),
- SPTS for Solenoid Packages and Current Leads,
- CMTS for assembled Cryomodules.

CONCLUSION

A set of new rod electrodes was installed in the SARAF RFQ. Following a short conditioning period acceleration of a 1mA CW deuteron beam has been demonstrated for the first time. All measured beam parameters agree with the design values [19].

The SARAF-LINAC project is approaching the end of the design stage and about to transition into the production

stage. All major components prototypes or first of series are being built or already being tested. The cryomodule design passed the CDR and the tendering process for its sub-components is about to commence.

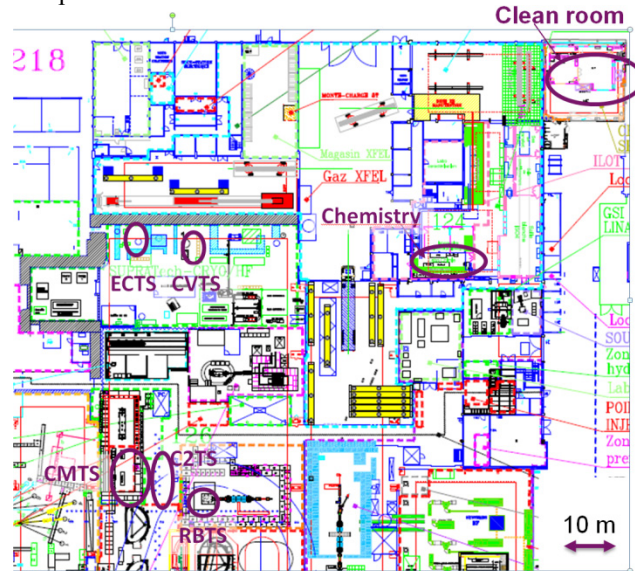


Figure 14: SARAF-LINAC Test Stands @ CEA-Saclay.

REFERENCES

- [1] A. Nagler et al., "Status of the SARAF Project", in Proc. LINAC'08, Victoria, Canada, Sep.-Oct. 2008, paper MO203, p. 26.
- [2] N. Pichoff et al., "The SARAF-LINAC project 2018 status", in Proc. 9th Int. Particle Accelerator Conf. (IPAC'18), Vancouver, Canada, Apr.-May 2018, p. 994, doi:10.18429/JACoW-IPAC2018-TUPAK015
- [3] P. Fischer et al., "Tuning a CW 4-Rod RFQ", in Proc. LINAC'06, Knoxville, Tennessee, USA, August 2006, p. 728.
- [4] J. Rodnizki et al., "SARAF 4-rod RFQ RF power Line splitting design and test", in Proc. LINAC'16, East Lansing, Michigan, USA, September 2016, p. 693.
- [5] A. Shor and A. Perry, "Redesign of SARAF RFQ Electrode Modulation to Enable CW Deuteron Operation at P=186 kW (HV=56 kV)", Internal SNRC report (2017), available per request.
- [6] General Particle Tracer (GPT) code, www.pulsar.nl
- [7] J. Dumas et al., "Beam dynamic studies for the SARAF MEBT and SCL", in Proc. IPAC'17, Copenhagen, Denmark, May 2017, p. 655.
- [8] CST Microwave Studio, www.cst.com.
- [9] L. Weissman et al., "First experience at SARAF with protons beam using Rutherford scattering monitor", in Proc. DIPAC'09, Basel, Switzerland, September 2009, p. 208.
- [10] J. Rodnizki et al., "Energy and Energy Spread Measurements using the Rutherford Scattering Technique for Tuning the SARAF Superconducting ", in Proc. LINAC'10, Tsukuba, Japan, September 2010, p. 620.
- [11] D. Uriot et al., "Status of TraceWIN code", in Proc. IPAC'15, Richmond, VA, USA, May 2015, p. 92, doi:10.18429/JACoW-IPAC2015-MOPWA008

- [12] P.A.P. Nghiem et al., “Strategy of Beam tuning implementation for the SARAF MEBT and SC Linac”, in Proc. IPAC’17, Copenhagen, Denmark, May 2017, p. 652.
- [13] See <http://www.sdms.fr>
- [14] See <http://www.research-instruments.de/>
- [15] See <https://etd.canon/>
- [16] See <http://www.elytt.com>
- [17] See <https://www.criotec.com>
- [18] N. Pichoff et al., “Discussion on SARAF-LINAC Cryomodules”, in Proc. HB’18, Daejeon, Korea, June 2018, p. 80, doi:10.18429/JACoW-HB2018-TUA2WC01
- [19] L. Weissman et al., “Installation and Commissioning of the Upgraded SARAF 4-rods RFQ”, in Proc. HB’18, Daejeon, Korea, June 2018, p. 75, doi:10.18429/JACoW-HB2018-TUA1WC01